Astron. Astrophys. 334, 498–504 (1998)

ASTRONOMY AND ASTROPHYSICS

Does the optical-to-X-ray energy distribution of quasars depend on optical luminosity?

W. Yuan, J. Siebert, and W. Brinkmann

Max-Planck-Institut für Extraterrestrische Physik, Giessenbachstrasse, D-85740 Garching, Germany

Received 18 September 1997 / Accepted 15 January 1998

Abstract. We report on a detailed analysis of the correlation between the optical-UV and X-ray luminosities of quasars by means of Monte Carlo simulations, using a realistic luminosity function. We find, for a quasar population with an intrinsically constant, mean X-ray loudness $\overline{\alpha}_{\rm ox}$, that the simulated $\alpha_{\rm ox} - L_{\rm o}$ relation can exhibit various 'apparent' properties, including an increasing $\overline{\alpha}_{\rm ox}$ with $L_{\rm o}$, similar to what has been found from observations. The determining factor for this behavior turns out to be the relative strength of the dispersions of the luminosities, i.e. their deviations from the mean spectral energy distribution at the optical and X-ray bands, such that a dispersion larger for the optical luminosity than for the X-ray luminosity tends to result in an apparent correlation. We suggest that the observed $\alpha_{\rm ox} - L_{\rm o}$ correlation can be attributed, at least to some extent, to such an effect, and is thus not an underlying physical property. The consequences of taking into account the luminosity dispersions in an analysis of the observed luminosity correlations is briefly discussed. We note that similar considerations might also apply for the Baldwin effect.

Key words: quasars: general – X-rays: general – methods: statistical

1. Introduction

A study of the dependence of the spectral energy distribution (SED) of quasars on their luminosity and/or on cosmic epoch is particularly important for understanding the quasar phenomenon. In the optical-to-X-ray regime, the SED can be characterized by the broad band spectral index between 2500Å and 2 keV, which is defined as $\alpha_{\rm ox} = -0.384 \log(L_{\rm 2keV}/L_{\rm 2500\AA})$. Quasars are known to exhibit strong luminosity evolution in the X-ray and the optical wave bands (e.g. Boyle 1994). However, there have been controversial discussions in the past as to whether the evolution law is the same in these two energy bands. A dependence of $\alpha_{\rm ox}$ on redshift or optical luminosity would indicate different evolution in the optical and the X-ray regime. Further, if $\alpha_{\rm ox}$ depends on optical luminosity, this is equivalent to a non-linear relationship between X-ray and optical luminosity ($L_{\rm x} \propto L_{\rm o}^{\rm e}$, $e \neq 1$).

Send offprint requests to: W. Yuan

While most of the analyses agree on the result that $\alpha_{\rm ox}$ is redshift independent, it has been claimed that $\alpha_{\rm ox}$ increases with $L_{\rm o}$, which implies that the objects with high optical luminosities are under-luminous in X-rays compared to their low luminosity counterparts (Avni & Tananbaum 1982, 1986; Kriss & Canizares 1985; Wilkes et al. 1994; Avni et al. 1995; Green et al. 1995). Generally, for a functional dependence of the form $\alpha_{\rm ox} \sim \beta \log L_{\rm o}$, a canonical slope of $\beta \sim 0.1$ was obtained, which is equivalent to a non-linear relation of the form $L_{\rm x} \propto L_{\rm o}^{0.7}$.

Based on Monte Carlo simulations, Chanan (1983) suggested that a non-linear relation might arise even for an intrinsically linear dependence from observational flux limits and the large intrinsic scatter in the data. Thus, the observed $\alpha_{\rm ox} - L_{\rm o}$ correlation should not be considered as an underlying physical reality. The author also claimed that the choice of $L_{\rm o}$ as the independent variable is not justified. However, Kriss & Canizares (1985) criticized these results by pointing out that they depend critically on the assumption of a Gaussian distribution for the luminosity functions.

A study by La Franca et al. (1995) reinforced the idea of a linear relationship between the X-ray and the optical luminosity for quasars. They applied a regression algorithm to a large sample of quasars detected with *Einstein*, which accounts for errors in both variables and the intrinsic scatter in the data, and found $L_{\rm x} \propto L_{\rm o}$.

In a recent study of ROSAT detected quasars by Brinkmann et al. (1997), it has been shown by means of a simple argument that an apparent correlation between $\alpha_{\rm ox}$ and $\log L_{\rm o}$ can indeed emerge even for intrinsically uncorrelated variables. Motivated by this idea, as well as by recent improvements concerning the shape of the quasar luminosity functions in the optical and the X-ray regime, we carry out a detailed study of this controversial problem by means of a Monte Carlo analysis. We mostly use the logarithms of luminosities and denote them as $l_{\rm x} = \log L_{\rm x}$ and $l_{\rm o} = \log L_{\rm o}$. We use $q_0 = 0.5$, $H_0 = 50\ {\rm kms}^{-1}{\rm Mpc}^{-1}$ throughout this paper. All errors quoted are at the 1σ level unless mentioned otherwise.

2. Analysis of luminosity correlations

2.1. Distribution of quasar luminosities

We first describe the assumed parametric form of the multivariate distribution $\psi(l_{\rm o}, l_{\rm x}, z)$, which we use in the simulations. In previous studies (e.g. Avni & Tananbaum 1982, 1986; Kriss & Canizares 1985) $\psi(l_{\rm o}, l_{\rm x}, z)$ is commonly expressed as the product of the luminosity function (LF hereafter) of the primary luminosity (either $l_{\rm x}$ or $l_{\rm o}$) and the conditional distribution function of the secondary luminosity. The conditional distribution function determines the expected value of the secondary luminosity by assuming a functional dependence between the two luminosities and intrinsic dispersion. In previous models, the dispersion of $\alpha_{\rm ox}$ was attributed to the dispersion in the secondary luminosity alone. In this paper we use a generalized description of the multivariate distribution function. We assume that both luminosities show intrinsic dispersion instead of the secondary luminosity only.

We introduce *intrinsic* optical and X-ray luminosities $\bar{l}_{\rm o}$ and $\bar{l}_{\rm x}$. The observed luminosities $l_{\rm o}$ and $l_{\rm x}$ are the intrinsic luminosities modified by various mechanisms which produce a large scatter. The luminosities $\bar{l}_{\rm o}$ and $\bar{l}_{\rm x}$ are distributed according to their respective luminosity functions, $\overline{\phi}_{\rm o}(\bar{l}_{\rm o}, z)$ and $\overline{\phi}_{\rm x}(\bar{l}_{\rm x}, z)$. Although $\bar{l}_{\rm o}$ and $\bar{l}_{\rm x}$ are not directly observable, their ratio, i.e. the *intrinsic* $\overline{\alpha}_{\rm ox}$, which is defined as

$$\overline{\alpha}_{\rm ox} \equiv -\frac{\bar{l}_{\rm o} - \bar{l}_{\rm x}}{\log(\nu_{2500\text{Å}}/\nu_{\rm 2keV})} = 0.384(\bar{l}_{\rm o} - \bar{l}_{\rm x}), \quad (1)$$

can be approximated by the mean of the observed $\alpha_{\rm ox}$ distribution. As indicated by the observed correlation between $l_{\rm x}$ and $l_{\rm o}$, $\bar{l}_{\rm x}$ and $\bar{l}_{\rm o}$ are physically related. Assuming a redshift-independent relationship of the form

$$\bar{l}_{\rm x} = f(\bar{l}_{\rm o}) \propto e\,\bar{l}_{\rm o}\,, \quad (2)$$

we get an *intrinsic* dependence of $\overline{\alpha}_{\rm ox}$ on $\bar{l}_{\rm o}$,

$$\overline{\alpha}_{\rm ox}(\bar{l}_{\rm o}) = \beta_{\rm int}\bar{l}_{\rm o} + \text{const}, \quad \text{where } \beta_{\rm int} = 0.384(1-e). \quad (3)$$

If $e = 1$, we have $\beta_{\rm int} = 0$, i.e. $\overline{\alpha}_{\rm ox}$ is independent of the luminosities *intrinsically*.

The *observed* optical and X-ray luminosities of a quasar are then

$$l_{\rm o} = \bar{l}_{\rm o} + \delta l_{\rm o}, \qquad l_{\rm x} = \bar{l}_{\rm x} + \delta l_{\rm x}, \quad (4)$$

where $\delta l_{\rm o}$ and $\delta l_{\rm x}$ quantify the scatter around the intrinsic luminosities in the optical and the X-ray band, respectively. The dispersion of $\alpha_{\rm ox}$ can now be attributed to the dispersions in both $l_{\rm x}$ and $l_{\rm o}$. Assuming that $\delta l_{\rm o}$ and $\delta l_{\rm x}$ are independent, we have[1]

$$(\delta\alpha_{\rm ox})^2 = 0.384^2\,[(\delta l_{\rm o})^2 + (\delta l_{\rm x})^2], \quad (5)$$

where $\delta\alpha_{\rm ox}$ is the dispersion of $\alpha_{\rm ox}$.

[1] In the general case $(\delta\alpha_{\rm ox})^2 = 0.384^2\,[e^2(\delta l_{\rm o})^2 + (\delta l_{\rm x})^2]$ with e from Eq. 2 and $e = 1 - \beta_{\rm int}/0.384$. If $e \sim 1$ then $\beta_{\rm int} \sim 0$. The same applies for $\sigma\alpha_{\rm ox}$ in Eq. 7.

Based on this generalized scenario, the multivariate distribution function $\psi(l_{\rm o}, l_{\rm x}, z)$ can be replaced by a distribution function depending on z, $\bar{l}_{\rm o}$, $\bar{l}_{\rm x}$, $\delta l_{\rm o}$ and $\delta l_{\rm x}$, which is given by

$$\psi^*(\bar{l}_{\rm o},\bar{l}_{\rm x}, \delta l_{\rm o}, \delta l_{\rm x}, z) = \overline{\phi}_{\rm o}(\bar{l}_{\rm o}, z)\,\delta(\bar{l}_{\rm x} - f(\bar{l}_{\rm o}))\,g_{\rm o}(\delta l_{\rm o}\,|\,\bar{l}_{\rm o}, z)\,g_{\rm x}(\delta l_{\rm x}\,|\,\bar{l}_{\rm o}, z), \quad (6)$$

where $\overline{\phi}_{\rm o}$ is the luminosity function for $\bar{l}_{\rm o}$, $\delta(\bar{l}_{\rm x} - f(\bar{l}_{\rm o}))$ is a δ-function with f from Eq. 2, and $g_{\rm o}$ and $g_{\rm x}$ are the conditional distribution functions for $\delta l_{\rm o}$ and $\delta l_{\rm x}$, respectively. In the following we describe these terms as they were implemented in the Monte Carlo analysis.

We assume that both luminosity dispersions, $\delta l_{\rm o}$ and $\delta l_{\rm x}$, are independent of luminosity and redshift, and that $g_{\rm o}$ and $g_{\rm x}$ are given by Gaussian distributions with means of zero, and standard deviations $\sigma_{\rm o}$ and $\sigma_{\rm x}$, respectively. Thus, the distribution of $\alpha_{\rm ox}$ is Gaussian with standard deviation

$$\sigma\alpha_{\rm ox} = 0.384\,({\sigma_{\rm o}}^2 + {\sigma_{\rm x}}^2)^{1/2}. \quad (7)$$

$\sigma\alpha_{\rm ox}$ is available from observational data, ranging from 0.15 to 0.2 (e.g. Avni et al. 1995, Yuan et al. 1998). We define the parameter R_σ as the ratio of the standard deviations of the optical to the X-ray luminosity dispersions,

$$R_\sigma \equiv \frac{\sigma_{\rm o}}{\sigma_{\rm x}}.$$

Then, given R_σ and $\sigma_{\alpha_{\rm ox}}$, $\sigma_{\rm o}$ and $\sigma_{\rm x}$ can be determined using Eq. 7.

Another input is the LF $\overline{\phi}_{\rm o}(\bar{l}_{\rm o}, z)$, which is not directly observable. Assuming a z-dependent power law for $\overline{\phi}_{\rm o}(\bar{l}_{\rm o}, z)$ and a Gaussian distribution for $g_{\rm o}$, it can be shown that the LF for the observed luminosity $l_{\rm o}$ has the same functional form and evolution as that for $\bar{l}_{\rm o}$ except close to the low-luminosity cutoff. Therefore, it is natural to approximate $\overline{\phi}_{\rm o}(\bar{l}_{\rm o}, z)$ by the observed optical luminosity function (OLF) and its evolution. If $\delta l_{\rm o}$ is small, $\overline{\phi}_{\rm o}(\bar{l}_{\rm o}, z)$ reduces to the observed OLF.

We assume pure luminosity evolution for quasars. Using the functional form of the OLF as given by Boyle (1994), which was derived from the UVX sample, we parameterize $\overline{\phi}_{\rm o}(\bar{l}_{\rm o}, z)$ by a broken power law with $\gamma_1 = -1.6$ for $\bar{l}_{\rm o} < l^*_{\rm o}$ and $\gamma_2 = -3.9$ for $\bar{l}_{\rm o} > l^*_{\rm o}$, and $\bar{l}^*_{\rm o}(z) = \bar{l}^*_{\rm o}(\text{z=0}) + k \cdot \log(1+z)$, $k \sim 3.5$, for $z < 2$. A low-luminosity cutoff was applied at $M_{\rm B}^{\rm min} = -20$ at $z = 0$ for $\bar{l}_{\rm o}$.

It should be noted that $\bar{l}_{\rm o}$ and $\bar{l}_{\rm x}$ are equivalent and interchangeable in this model. Eq. 6 can also be expressed in terms of $\bar{l}_{\rm x}$, in which case the X-ray luminosity function (XLF) has to be used instead of OLF.

2.2. Monte Carlo analysis

The Monte Carlo analysis was performed by generating a sample of quasars with z, $l_{\rm o}$, and $l_{\rm x}$ as follows:
First, a redshift z was drawn from a given range (z_1, z_2) satisfying $V(z_1, z)/V(z_1, z_2) = r_1$, where $V(z_1, z)$ and $V(z_1, z_2)$ are the volumes within (z_1, z) and (z_1, z_2), respectively, and r_1

is a random number between 0 and 1. The volume element in co-moving space is given by (for $q_0 = 0.5$)

$$dV(z) = 16\pi(c/H_0)^3(1+z)^{-3.5}(1+z-\sqrt{1+z})^2\,dz. \quad (8)$$

Then, a second random number r_2 was calculated and the intrinsic luminosity at the optical band $\overline{l}_{\rm o}$ was determined such that $\int_{\overline{L}_{\rm o}^{\rm min}}^{\overline{L}_{\rm o}} \overline{\phi}_{\rm o}(\overline{L'}_{\rm o}, z)\,d\overline{L'}_{\rm o} \,/\, \int_{\overline{L}_{\rm o}^{\rm min}}^{\infty} \overline{\phi}_{\rm o}(\overline{L'}_{\rm o}, z)\,d\overline{L'}_{\rm o} = r_2$, with the luminosity function $\overline{\phi}_{\rm o}(\overline{L}_{\rm o}, z)$ as specified above. After that, the expected X-ray luminosity $\overline{l}_{\rm x}$ was obtained using Eq. 1 for a given $\overline{\alpha}_{\rm ox}$. The *observed* optical and X-ray luminosities, $l_{\rm o}$ and $l_{\rm x}$, are then drawn from the Gaussian distribution functions $g_{\rm o}(l_{\rm o} - \overline{l}_{\rm o})$ and $g_{\rm x}(l_{\rm x} - \overline{l}_{\rm x})$, respectively. The corresponding fluxes were calculated from the luminosities assuming $\alpha_{\rm o} = -0.5$ and $\alpha_{\rm x} = -1.3$ for the K-corrections, respectively. An object was accepted, if the fluxes were above the given flux limits. In general we simulated optically selected samples assuming a threshold magnitude $m_{\rm B,th}$ = 20. If the objects turned out to have an X-ray flux below the assumed X-ray flux limit they were treated as 'non-detections'.

The above procedure was repeated until a sample comprising 300 objects was obtained. For each object, $\alpha_{\rm ox}$ was calculated from the simulated $l_{\rm o}$ and $l_{\rm x}$. We then investigated the $\alpha_{\rm ox} - l_{\rm o}$ relationship by means of a Spearman rank correlation test and least-square linear regression analysis. For a specific set of parameters of the quasar population, we carried out 10 independent trials and acquired 10 samples. All statistical quantities derived below are the mean of the individual values of the 10 samples, along with the statistical uncertainty for the mean.

2.3. Results

As the first and simplest case we assumed the intrinsic $\overline{\alpha}_{\rm ox}$ and $\sigma_{\alpha_{\rm ox}}$ in Eqs. 3 and 7 to be constant, i.e. independent of luminosity. In accordance with observational results we used $\overline{\alpha}_{\rm ox} = 1.40$ and $\sigma_{\alpha_{\rm ox}} = 0.18$. We considered 20 values of the R_σ-parameter from $R_\sigma = 0.1$ to 10, which are sampled evenly on a logarithmic scale. Eq. 7 then determines the dispersions $\sigma_{\rm o}$ and $\sigma_{\rm x}$. We investigated optically selected samples with a size of $N = 300$ and a limiting magnitude $m_{B,\rm th} = 20$. In a first attempt, we restrict our analysis to samples at a fixed redshift ($z = 1$), for which the results give an insight into the physical problem, and then we present cases for samples in larger redshift ranges.

2.3.1. Sample at fixed redshift

The Spearman correlation coefficients $\rho_{\rm sp}$ are plotted in Fig. 1 as open squares for 20 different R_σ values, with the typical 1σ error indicated for illustration. The probability levels $P_r = 0.01$ and 0.001, at which the 'no correlation' hypothesis is ruled out, are shown at the corresponding $\rho_{\rm sp}$ ($N = 300$) as dotted and dashed lines, respectively. Despite of the luminosity independence of the intrinsic mean $\overline{\alpha}_{\rm ox}$ the results show the emergence of a positive correlation with increasing R_σ, which becomes significant for $R_\sigma > 1$. In Fig. 2 we show an example of an $\alpha_{\rm ox}$ versus $l_{\rm o}$ plot for a simulated sample with $R_\sigma = 5$. The dashed line represents a constant X-ray luminosity ($l_{\rm x}$ = 27.2 erg s^{-1} Hz^{-1}). Obviously, the simulation indicates a much sharper cutoff in X-ray luminosity compared to optical luminosity, which has already been noted by Brinkmann et al. (1997) for observed data.

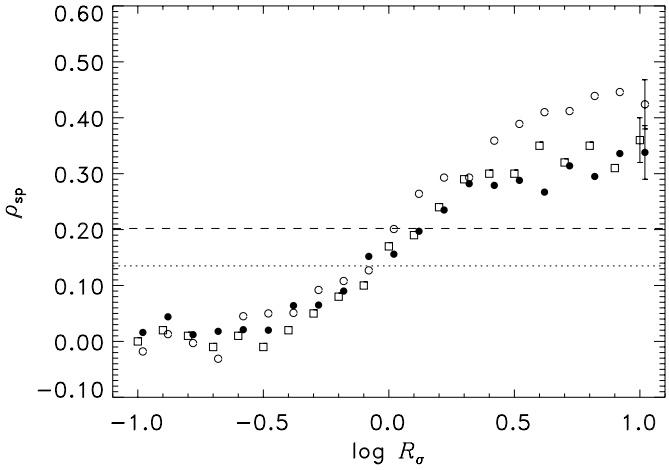

Fig. 1. Spearman rank correlation coefficients $\rho_{\rm sp}$ as a measure of the $\alpha_{\rm ox} - l_{\rm o}$ correlation for simulated samples for various R_σ-parameters; squares: sample at fixed redshift; filled circles: sample with redshift $0.2 < z < 3$; open circles: sample with redshift $0.2 < z < 3$ and containing only X-ray detections. The dotted and dashed lines indicate the $\rho_{\rm sp}$ for which the 'no correlation' hypothesis can be ruled out at the corresponding probability levels (one tail) of 0.01 and 0.001, respectively.

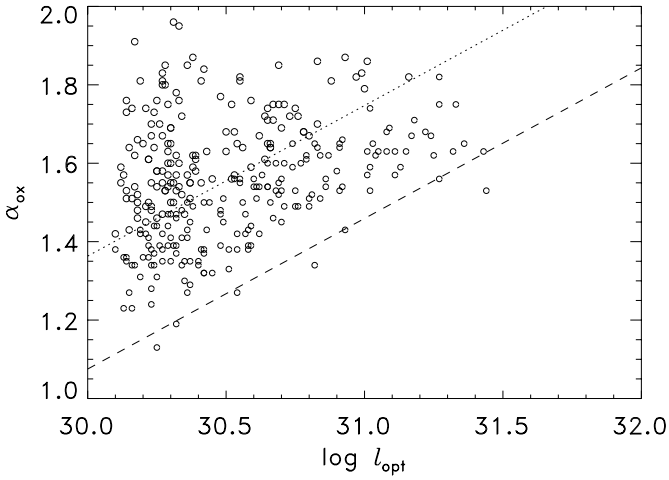

Fig. 2. $\alpha_{\rm ox}$ versus $l_{\rm o}$ for a simulated quasar sample at $z = 1.0$, assuming a constant $\overline{\alpha}_{\rm ox}$ and $R_\sigma = 5$. The lines indicate constant X-ray luminosities, $l_{\rm x} = 27.2\,{\rm erg\,s^{-1}\,Hz^{-1}}$ (dashed) and $l_{\rm x} = 26.5\,{\rm erg\,s^{-1}\,Hz^{-1}}$ (dotted).

Now we consider the effects of thresholds in the X-ray observations. At a redshift of z=1 a luminosity threshold of $l_{\rm x}^{\rm th} \sim 26.5\,{\rm erg\,s^{-1}\,Hz^{-1}}$ at 2 keV indicated by the dotted line in Fig. 2 corresponds to a flux limit of $\sim 4\times10^{-14}\,{\rm erg\,cm^{-2}\,s^{-1}}$ in the 0.5-2 keV band. Objects below this line have $l_{\rm x} \geq l_{\rm x}^{\rm th}$ and can thus be 'detected' in X-rays; whereas the rest with $l_{\rm x} < l_{\rm x}^{\rm th}$ are 'non-detections'. When only the 'detections' are consid-

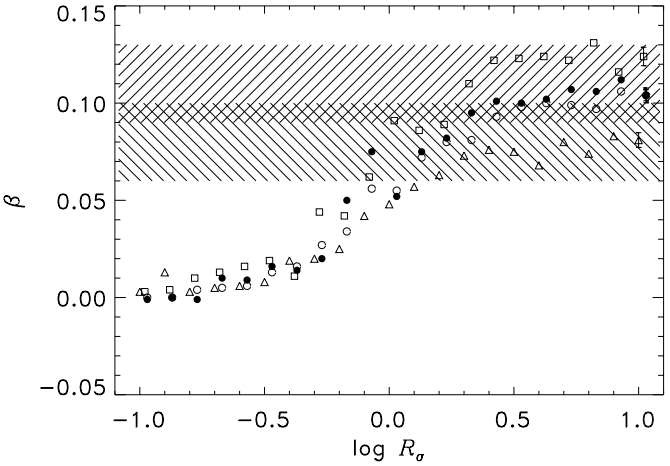

Fig. 3. Fitted slopes of $\alpha_{\rm ox} \sim \beta \log L_{\rm o}$ for various R_σ values. Filled circles: no X-ray threshold considered and $\sigma_{\alpha_{\rm ox}} = 0.18$; open circles: with X-ray threshold and $\sigma_{\alpha_{\rm ox}} = 0.18$; triangles: with X-ray threshold and $\sigma_{\alpha_{\rm ox}} = 0.15$; squares: with X-ray threshold and $\sigma_{\alpha_{\rm ox}} = 0.20$. The two shaded areas indicate the typical range of slopes ($1\,\sigma$) given in two previous studies (see text).

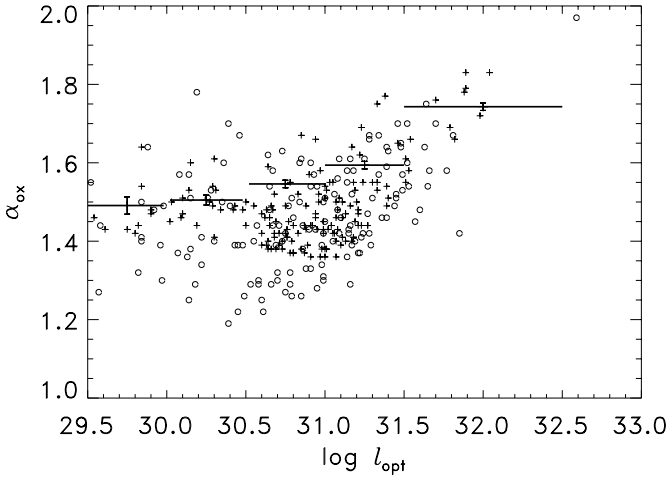

Fig. 4. $\alpha_{\rm ox}$ versus $\log L_{\rm o}$ for a simulated quasar sample in the redshift range $0.2 < z < 3$, assuming $R_\sigma = 5$. Crosses indicate lower limits for objects which would not have been detected in the presence of an observational X-ray threshold. Thick bars indicate the best estimates of the mean $\alpha_{\rm ox}$ in $l_{\rm o}$ bins which were obtained by taking into account non-detections (see Sect. 3.2).

ered[2], the X-ray thresholds can enhance the apparent $\alpha_{\rm ox} - l_{\rm o}$ correlation significantly, as can be inferred from the figure.

The results are independent of redshift, which changes only the range of optical luminosities.

2.3.2. Samples in redshift ranges

We now consider samples with a redshift range of $0.2 < z < 3.0$. The results of the correlation analysis are added to Fig. 1 for the case without (filled circles) and with an X-ray threshold (open circles). We find almost the same results as for the sample at fixed redshift.

The slopes β obtained by fitting a linear $\alpha_{\rm ox} \sim \beta \cdot l_{\rm o}$ relation to the simulated samples, are plotted in Fig. 3 for various R_σ values, for the case without (filled circles) and with (open circles) X-ray thresholds, respectively. The results are fully consistent with those of the rank correlation test. Another effect to be noted is that the resulting average $\alpha_{\rm ox}$ of the obtained sample is consistent with the intrinsic $\overline{\alpha}_{\rm ox}$ ($= 1.4$) only for small R_σ ($\ll 1$), and it increases towards higher R_σ with a typical difference of ~ 0.1 for $R_\sigma \gg 1$.

The fitted slopes are found to be independent of the specified value of $\overline{\alpha}_{\rm ox}$ and insensitive to the X-ray observational thresholds as well as to sample completeness. However, they depend slightly on the dispersion $\sigma_{\alpha_{\rm ox}}$ (within plausible limits on $\sigma_{\alpha_{\rm ox}}$) in a manner that, at large R_σ, the slope increases with $\sigma_{\alpha_{\rm ox}}$ for a given R_σ. We plot in Fig. 3 the results for samples assuming $\sigma_{\alpha_{\rm ox}} = 0.15$ (triangles) and $\sigma_{\alpha_{\rm ox}} = 0.2$ (squares), respectively, ignoring the effect of X-ray thresholds. The shaded areas in the figure indicate the 1σ confidence region of β obtained in previous studies ($\beta_{\rm obs} = 0.11 \pm 0.02$, Wilkes et al. 1994, Yuan et al. 1998; $\beta_{\rm obs} = 0.08 \pm 0.02$, Green et al. 1995). It shows that the observed slopes can be reproduced within a relatively large region in the parameter space of R_σ and $\sigma_{\alpha_{\rm ox}}$. Furthermore, the slopes also depend only marginally on the low-luminosity cutoff $M_{\rm B}^{\rm min}$ chosen for $\overline{l}_{\rm o}$, which is somewhat uncertain.

In Fig. 4 we show the simulated $\alpha_{\rm ox}$ and $l_{\rm o}$ values for $R_\sigma = 5$. For 'non-detections' lower limits on $\alpha_{\rm ox}$ are shown as crosses. This distribution, as well as that for samples at fixed redshift (Fig. 2), differs from what is expected for a linear $\alpha_{\rm ox} \sim l_{\rm o}$ relation, showing asymmetric structures with respect to a regression line.

To test the correctness of the simulation procedure each sample was subjected to a self-consistency check using the evolution weighted Schmidt's (1968) $V/V_{\rm m}$, as in Chanan (1983). The simulated samples represented the envisaged luminosity function evolution as the resulting $\langle V/V_{\rm m} \rangle$ were distributed randomly around 0.5 within the $1\,\sigma$ uncertainties.

We also performed similar analyses starting from $\overline{l}_{\rm x}$ instead of $\overline{l}_{\rm o}$. After having determined z, $\overline{l}_{\rm x}$ was drawn from the LF for $\overline{l}_{\rm x}$, $\overline{\phi}_{\rm x}(\overline{l}_{\rm x}, z)$, which is approximated by the observed XLF. We used the broken power law LF as given in Boyle (1994), with a faint-end slope $\gamma_1 = -1.6$, a bright-end slope $\gamma_2 = -3.3$, and evolution rate $k = 3.3$ for $z < 2$. Then, a corresponding $\overline{l}_{\rm o}$ was obtained from Eq. 1 for the given $\overline{\alpha}_{\rm ox}$. The observed luminosities were drawn in the same way as above. Similar results were found, i.e. an apparent $\alpha_{\rm ox} - l_{\rm o}$ correlation towards high R_σ. This is expected because of the striking similarity between the OLF and XLF (Boyle 1994).

We conclude that an apparent $\alpha_{\rm ox} - l_{\rm o}$ correlation can emerge even for a population with an intrinsically constant $\overline{\alpha}_{\rm ox}$ in the presence of large dispersions in the SED and for $R_\sigma \geq 1$. The degree of correlation depends on the R_σ-parameter. Similar

[2] Hereafter, we refer to such a case as 'with an X-ray threshold', otherwise we refer to data 'without an X-ray threshold'

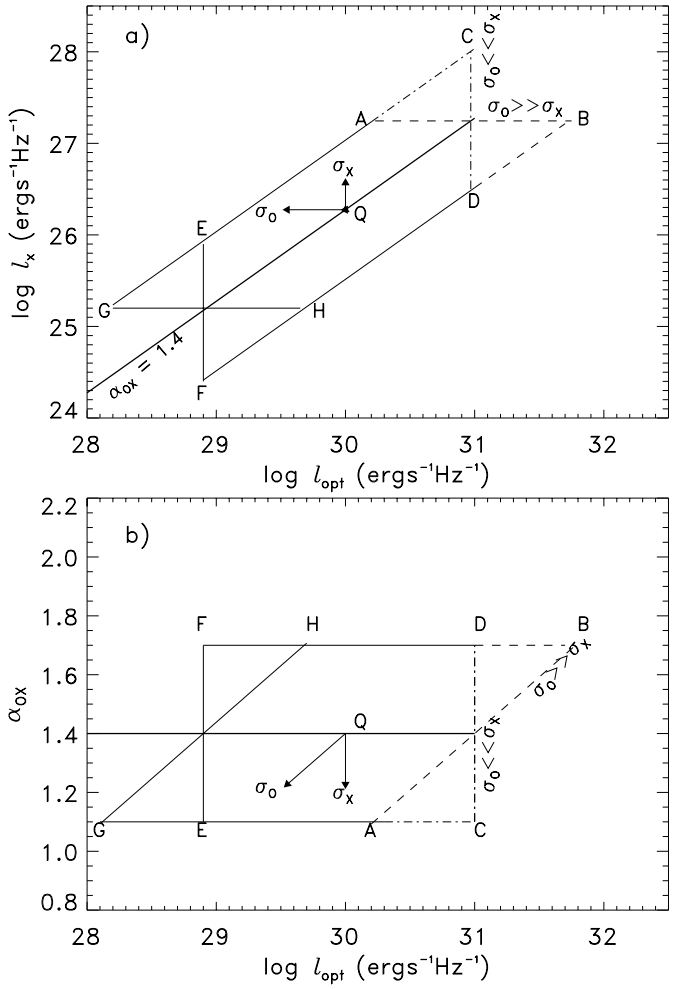

Fig. 5a and b. Schematic sketches for the $l_{\rm x}-l_{\rm o}$ and $\alpha_{\rm ox}-l_{\rm o}$ relationship. See text for a detailed explanation of the various symbols.

results hold for X-ray selected quasar samples, as well as for incomplete samples.

3. Discussion

3.1. Intuitive consideration

The simulation results can be understood in terms of simple intuitive arguments. We show schematic sketches for the $l_{\rm x}-l_{\rm o}$ relation in Fig. 5a and the corresponding $\alpha_{\rm ox}-l_{\rm o}$ relation in Fig. 5b for a sample at fixed redshift. Following Sect. 2.1, the distribution of luminosities in the optical and X-ray regime is determined by the mean $\overline{\alpha}_{\rm ox}$. A constant $\overline{\alpha}_{\rm ox}=1.4$ is assumed (thick lines in Figs. 5a and b), as well as constant luminosity dispersions $\sigma_{\rm o}$ and $\sigma_{\rm x}$ (indicated for an object at Q). The expected luminosities $\bar{l}_{\rm o}$ and $\bar{l}_{\rm x}$ are distributed along the line of constant $\overline{\alpha}_{\rm ox}$ according to their distribution function $\overline{\phi}_{\rm o}(\bar{l}_{\rm o}(\bar{l}_{\rm x}),z)$, with a cutoff at the bright end of $\bar{l}_{\rm o}$ and $\bar{l}_{\rm x}$ for a sample with finite size.

We consider the distribution of objects deviating from $\bar{l}_{\rm o}$ and $\bar{l}_{\rm x}$ due to luminosity scatter in the $l_{\rm x}-l_{\rm o}$ and $\alpha_{\rm ox}-l_{\rm o}$ planes. The 90% probability region for an object is confined within the two thin lines parallel to the mean $\overline{\alpha}_{\rm ox}$. We consider two extreme cases: $\sigma_{\rm o}\gg\sigma_{\rm x}$ ($R_\sigma\gg1$) and $\sigma_{\rm o}\ll\sigma_{\rm x}$ ($R_\sigma\ll1$). For $\sigma_{\rm o}\gg\sigma_{\rm x}$, the luminosity scatter is predominant in the optical luminosity, i.e. along the optical axis. The distribution of objects in the $l_{\rm x}-l_{\rm o}$ plane forms a confined region below the horizontal dashed line AB, which corresponds to the line AB with slope 0.384 in Fig. 5b. An apparent correlation appears between $\alpha_{\rm ox}$ and $l_{\rm o}$ for such distributions, despite the intrinsically uncorrelated relation. This effect explains the simulated $\alpha_{\rm ox}-l_{\rm o}$ distribution in Fig. 2. On the other hand, in the case of $\sigma_{\rm o}\ll\sigma_{\rm x}$, objects are distributed in a region confined by line CD (dashed-dotted) and no $\alpha_{\rm ox}-l_{\rm o}$ correlation is expected from the high-$l_{\rm o}$ end. The actual degree of correlation increases with $\sigma_{\rm o}$ relative to $\sigma_{\rm x}$, which explains the dependence $\alpha_{\rm ox}-l_{\rm o}$ correlation on R_σ, as seen in Figs. 1 and 3. Moreover, flux limits in X-rays (indicated by the line GH), tend to enhance the apparent $\alpha_{\rm ox}-l_{\rm o}$ correlation, as can be seen from Fig. 5b and Fig. 2. For an optically selected sample, the cutoff due to the optical flux limit (indicated by EF) systematically excludes objects with smaller $\alpha_{\rm ox}$ values, which qualitatively explains the resulting increase of average $\alpha_{\rm ox}$ for large R_σ.

We note that, in order to get a sharply confined $\alpha_{\rm ox}-l_{\rm o}$ distribution at the high luminosity cutoffs, a steep luminosity function for $\bar{l}_{\rm o}$ ($\bar{l}_{\rm x}$) is required towards the high luminosity end. Our simulations show that the observed optical and X-ray quasar luminosity functions satisfy this condition.

Using simulations basically similar to ours and a much steeper luminosity function (Gaussian distribution), Chanan (1983) found the existence of a $\alpha_{\rm ox}-l_{\rm o}$ correlation in his cases B and C, but not in case A, corresponding to $R_\sigma\sim1.4$, $R_\sigma=1$, and $R_\sigma\sim0.8$ in our analysis. These values are close to the critical point $R_\sigma=1$, and the results of Chanan are thus not a consequence of the reversal of dependent and independent variables in the regression analysis. Furthermore, the use of the R_σ-parameter in our work, i.e. the relative strength of $\sigma_{\rm o}$ and $\sigma_{\rm x}$, is physically more meaningful than the assumption that the luminosity of one wave band directly determines that in the other band (as in Chanan 1983). The case of $R_\sigma\gg1$ leads to a more pronounced high-luminosity cutoff for $l_{\rm x}$ compared to $l_{\rm o}$ (see also Fig. 2). This effect is also seen in observational data (Brinkmann et al. 1997).

It can also be seen in Fig. 5a that, when performing a linear regression analysis for the $l_{\rm x}-l_{\rm o}$ relation, different distributions of the data near the highest luminosities can result in different slopes for different R_σ. Thus, a simple linear regression analysis method is not always adequate to quantify a luminosity correlation, especially for data with large inherent scatter.

3.2. Dependence of $\alpha_{\rm ox}$ on $l_{\rm o}$ – intrinsic or apparent?

Our results show that an apparent dependence of $\alpha_{\rm ox}$ on $l_{\rm o}$ can emerge from data for a quasar sample with no intrinsic dependence. Thus, the explanation of the observed $\alpha_{\rm ox}\sim l_{\rm o}$ correlation as a physical relation in quasars, as taken for granted in previous work, must be questioned. Although the current study does not allow to unambiguously distinguish between an *intrin-*

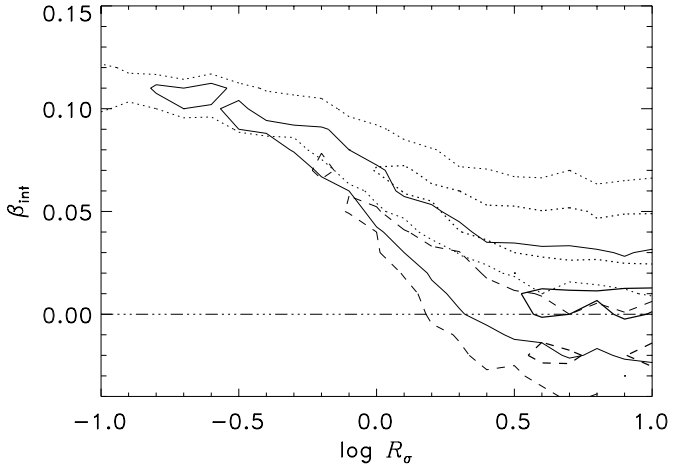

Fig. 6. Contours of the 68% (thick lines) and 90% (thin lines) confidence region in R_σ and $\beta_{\rm int}$, the slope of the intrinsic $\alpha_{\rm ox}-l_{\rm o}$ dependence, for $\sigma_{\alpha_{\rm ox}}=0.15$ (dotted), $\sigma_{\alpha_{\rm ox}}=0.18$ (solid) and $\sigma_{\alpha_{\rm ox}}=0.20$ (dashed).

sic or an *apparent* dependence of $\alpha_{\rm ox}$ on $l_{\rm o}$, we may reach some conclusions by simple considerations.

If our model is a good description of the quasar luminosity correlation and dispersion, we expect the existence of an apparent correlation to some extent, unless in cases of rather small R_σ ($\lesssim 0.3$), i.e. when the dispersion in $l_{\rm o}$ is at least 3 times less than that in $l_{\rm x}$, which seems unlikely considering the diversity of the big-blue-bump component in quasar energy spectra. In fact, the aforementioned characteristics of a much tighter high-luminosity cutoff for $l_{\rm x}$ than for $l_{\rm o}$ seems to exist in most quasar samples of considerable size. Thus, an intrinsic $\alpha_{\rm ox}-l_{\rm o}$ dependence, if it does exist, must be weaker than it appears from the data.

To quantify these effects, we carried out similar simulations incorporating an intrinsic luminosity dependent $\overline{\alpha}_{\rm ox}$ as in Eq. 3, $\beta_{\rm int}\neq 0$, and compare the obtained slopes β of the $\alpha_{\rm ox}-l_{\rm o}$ relation with the observed values. For each grid point in the $\beta_{\rm int}-R_\sigma$ parameter space, we repeated the simulations for 200 trials and counted the number m of trials for which β fell into a region around the observed value $\beta_{\rm obs}\pm u_\xi\sigma$, at a confidence level ξ. The overall confidence level of reproducing the observed slope is thus $\xi\cdot m/200$, if systematic uncertainties, such as sample incompleteness etc., are ignored. For $\beta_{\rm obs}=0.11\pm0.02$ (Wilkes et al. 1994, Yuan et al. 1998), Fig. 6 shows the contours of the 68% (thick lines) and 90% (thin lines) confidence regions of the joint $\beta_{\rm int}-R_\sigma$ distribution for $\sigma_{\alpha_{\rm ox}}=0.15$ (dotted), 0.18 (solid), and 0.20 (dashed), respectively. The results show that only a weak dependence ($\beta_{\rm int}\lesssim 0.05$) is needed for $R_\sigma\gtrsim 1$, when the dispersion in $l_{\rm o}$ is comparable to or larger than that in $l_{\rm x}$; and almost no intrinsic dependence is needed for larger $R_\sigma\gtrsim 3$. It also shows that the most probable (68%) region appears at high R_σ ($\gtrsim 1$), low $\beta_{\rm int}(\lesssim 0.07)$ values.

More qualitative evidence comes from some features of the observed $\alpha_{\rm ox}-l_{\rm o}$ relation. Recent studies of large quasar samples (Avni et al. 1995, Brinkmann et al. 1997, Yuan et al. 1998) have shown that the observed $\alpha_{\rm ox}-l_{\rm o}$ correlation shows a more complex behavior, with only weak or even vanishing correlation at low optical luminosities. We find that such features are expected, as the apparent correlation for $R_\sigma>1$ arises mainly from objects with high optical luminosities. This property has been verified by estimating the average $\alpha_{\rm ox}$ in different $l_{\rm o}$ bins for the simulated data. This can be seen in Fig. 4, where we plot the average $\alpha_{\rm ox}$ (thick bars) for five $l_{\rm o}$ bins, which were obtained by incorporating upper limits for the 'non detections' using the maximum likelihood method developed by Avni et al. (1980).

A comparison of the observed OLF and XLF and their evolution may also give, in principle, constraints on the intrinsic $\overline{\alpha}_{\rm ox}-\bar{l}_{\rm o}$, or $\bar{l}_{\rm x}-\bar{l}_{\rm o}$ relation (Eqs. 2 and 3). For a power law luminosity function for $\overline{L}_{\rm o}$ with index $\gamma_{\rm o}$, and luminosity evolution $\sim(1+z)^{k_{\rm o}}$, it can be shown (see also Kriss & Canizares 1985) that the corresponding LF for $\overline{L}_{\rm x}$ is also a power law (index $\gamma_{\rm x}$) with evolution $(1+z)^{k_{\rm x}}$ and

$$\gamma_{\rm x}-1=(\gamma_{\rm o}-1)/e,\qquad k_{\rm x}=ek_{\rm o}. \tag{9}$$

For a Gaussian approximation of the luminosity dispersion, the luminosity functions $\overline{\phi}_{\rm o}(\bar{l}_{\rm o},z)$, $\overline{\phi}_{\rm x}(\bar{l}_{\rm x},z)$ have the same forms and evolution as the observed luminosity functions $\phi_{\rm o}(l_{\rm o},z)$, $\phi_{\rm x}(l_{\rm x},z)$. Thus, e and $\beta_{\rm int}$ can be estimated from the observed $k_{\rm o}$, $k_{\rm x}$, $\gamma_{\rm o}$ and $\gamma_{\rm x}$.

The optical evolution index is found to be $k_{\rm o}=3.45\pm0.1$ (Boyle 1994). However, the X-ray evolution index is somewhat uncertain–ranging from $k_{\rm x}=2.56\pm0.17$ (Della Ceca et al. 1992, $q_0=0$, *Einstein* EMSS data only), $k_{\rm x}=3.0^{+0.2}_{-0.3}$ (Jones et al. 1997) and $k_{\rm x}=3.34\pm0.1$ (Boyle et al. 1994) to $k_{\rm x}=3.2-3.5$ (Franceschini et al. 1994). The latter three values were obtained by incorporating ROSAT data, and they are consistent with $e=1$ and $\beta_{\rm int}=0$ within their 2 σ errors, i.e. no intrinsic dependence of $\alpha_{\rm ox}$ on $l_{\rm o}$ is needed. Even if we take the smallest value of $k_{\rm x}=3.0$ of Jones et al. (1997), we have $e=0.87$ and $\beta_{\rm int}=0.05$, implying only a marginal dependence, weaker than the previous claims of $\beta\sim0.1$. The bright-end slopes of the XLF ($\gamma_2=3.30^{+0.34}_{-0.09}$) and of the OLF ($\gamma_2=3.9\pm0.1$, Boyle 1994) are consistent with each other within their 2σ errors, and thus also consistent with $e=1$ and $\beta_{\rm int}=0$. We conclude that a constant $\overline{\alpha}_{\rm ox}$ independent of $l_{\rm o}$ is not ruled out by a comparison of the observed luminosity functions in the optical and the X-ray band.

4. Conclusions

We have performed Monte Carlo simulations to study the luminosity correlation between the optical and X-ray bands for quasars. We have used a generalized model in which the luminosities in the two wave bands are represented in terms of the respective expected luminosities with dispersions ($l_{\rm o}=\bar{l}_{\rm o}+\delta l_{\rm o}$, $l_{\rm x}=\bar{l}_{\rm x}+\delta l_{\rm x}$). We have shown that the increase of $\alpha_{\rm ox}$ with $L_{\rm o}$ (equivalent to $L_{\rm x}\propto L_{\rm o}^e$ with $e<1$), as found in observational data, can emerge in a sample with an intrinsic luminosity independent $\alpha_{\rm ox}$ (or $L_{\rm x}\propto L_{\rm o}$), provided that the dispersion of the optical luminosities deviating from the average SED are similar to or larger than that of the X-ray luminosities. Our simulations

verified the results of Chanan (1983), which were achieved for special assumption about the luminosity functions. We suggest that the *observed* $\alpha_{\rm ox} - L_{\rm o}$ correlation is, at least to a large extent, apparent and not necessarily an intrinsic property of the quasar population.

Our model is more general than previous considerations. For $R_\sigma \ll 1$ (implying $l_{\rm o} \sim \bar{l}_{\rm o}$ and $\sigma_{\alpha_{\rm ox}} \sim 0.384\sigma_{\rm x}$) the model reduces to the commonly used description, in which $l_{\rm o}$ is the primary luminosity and the dispersion in the SED is attributed to that in the X-ray luminosity. The same holds for $R_\sigma \gg 1$, but with interchanged roles of $l_{\rm o}$ and $l_{\rm x}$. We argue that the effect of the relative strength of the individual luminosity dispersions in the two bands should be taken into account in analyses of quasar luminosity correlations. Since the arguments are valid for any other two wave bands, we expect this effect to play a role in luminosity correlations between radio, infrared, optical, and X-ray wave bands as well. The determination of the R_σ-parameter, and thus of the luminosity scatter in the individual wave bands, is important to understand the broad band emission of quasars.

We finally note that a similar effect as presented for the $\alpha_{\rm ox} - l_{\rm o}$ correlation might also apply for the well-known Baldwin effect, i.e. the inverse correlation of optical emission line equivalent width with optical luminosity (Baldwin 1977). Since the equivalent width basically can be regarded as the ratio of two luminosities (emission line and underlying continuum), the structure of the problem is similar to the one presented in this paper. This is particularly interesting, because there still is no accepted physical explanation for the Baldwin effect.

References

Avni Y., Tananbaum H., 1982, ApJ 262, L17
Avni Y., Tananbaum H., 1986, ApJ 305, 83
Avni Y., Soltan A., Tananbaum H., Zamorani G., 1980, ApJ 238, 800
Avni Y., Worrall D.M., Morgan, Jr. W.A., 1995, ApJ 454, 673
Baldwin J.A., 1977, ApJ 214, 679
Boyle B.J., 1994, in *The nature of compact objects in active galactic nuclei*, eds Robinson A. & Terlevich R., Cambridge Univ. press, p110
Boyle B.J., Shanks T., Georgantopoulos I., et al., 1994, MNRAS 271, 639
Brinkmann W., Yuan W., Siebert J., 1997, A&A 319, 413
Chanan G.A., 1983, ApJ 275, 45
Della Ceca R., Maccacaro T., Gioia I.M., et al., 1992, ApJ 389, 491
Franceschini A., La Franca F., Christiani S., Martin-Mirones J.M., 1994, MNRAS 269, 683
Green P.J., Schartel N., Anderson S.F., et al., 1995, ApJ 450, 51
Jones L.R., McHardy I.M., Merrifield M.R., et al. 1997, MNRAS 285, 547
Kriss G.A., Canizares C.R., 1985, ApJ 297, 177
La Franca F., Franceschini A., Christiani S., Vio R., 1995, A&A 299, 19
Schmidt M., 1968, ApJ 151, 393
Wilkes B.J., Tananbaum H., Worrall D., et al., 1994, ApJS 92, 53
Yuan W., Brinkmann W., Siebert J., Voges W., 1998, A&A 330, 108